Comparison of the Non-linear Spin Dynamics in Antiferromagnetic Chain Compounds Na2MnF5 and (ND4)2MnF5

ARTICLE *in* ZEITSCHRIFT FÜR ANORGANISCHE UND ALLGEMEINE CHEMIE · JUNE 2004

Impact Factor: 1.16 · DOI: 10.1002/zaac.200400009

Comparison of the Non-linear Spin Dynamics in Antiferromagnetic Chain Compounds Na_2MnF_5 and $(ND_4)_2MnF_5$

Jürgen Pebler[a,*], Christoph Frommen[a], Mathias Mangold[a], Ronald Stief[a], Alexander Krimmel[b], Reiner van de Kamp[c], Michael Ohl[d], and Louis-Pierre Regnault[e]

[a] Marburg, Fachbereich Chemie der Philipps-Universität und Wissenschaftliches Zentrum für Materialwissenschaften
[b] Augsburg,Universität Augsburg, Experimentelle Physik V
[c] Berlin, Hahn Meitner Institut, Abt. NI
[d] Jülich, Forschungszentrum Jülich, Institut für Festkörperforschung
[e] Grenoble / France, Centre d'Etudes Nuclèaires

Received January 16th, 2004.

Professor Werner Massa zum 60. Geburtstag gewidmet

Abstract. $Na_2Mn_{0.98}Fe_{0.02}F_5$ and $(ND_4)_2Mn_{0.98}Fe_{0.02}F_5$ was studied with the aid of Mössbauer spectroscopy. These results were interpreted on the basis of classical soliton theory. In order to confirm this concept, we have performed neutron scattering experiments on large single crystals of the pure compounds. We discuss the results obtained on a thermal and cold three-axis spectrometer, which probe the magnon spin wave excitations and the existence of the nonlinear excitations in the quasi 1-d antiferromagnetic chains of Na_2MnF_5 and $(ND_4)_2MnF_5$, respectively. Additionally, we include elastic neutron diffraction and dc. single crystal susceptibility measurements to determine the magnetic structure. From the width of the quasielastic scattering signal the temperature dependence of the inverse magnetic correlation lengths was derived resulting in a soliton activation energy ofE_s/k = 65(3) K and E_s/k = 81(3) K, respectively, which are in good agreement with the soliton energies obtained by our high resolution inelastic neutron scattering experiment. In contrast to these results the Mössbauer spectroscopy gives twice the value of the soliton energy caused by soliton pair or interband excitations.

Keywords: Fluoromanganate(III); Mössbauer spectroscopy; Magnetic susceptibility; Neutron scattering (inelastic and elastic); Magnon excitations; Nonlinear excitations

Vergleich der nichtlinearen Spindynamik in den antiferromagnetischen Kettenverbindungen Na_5MnF_5 und $(ND_4)_2MnF_5$

Inhaltsübersicht. Das spin-dynamische Verhalten der magnetisch eindimensionalen Verbindungen von $Na_2Mn_{0.98}Fe_{0.02}F_5$ and $(ND_4)_2Mn_{0.98}Fe_{0.02}F_5$ studierten wir mit Hilfe der Mössbauer Spektroskopie. Die erzielten Ergebnisse der Relaxation wurden auf der Basis der klassischen Solitonentheorie interpretiert. Zur Überprüfung dieses Konzepts haben wir Neutronenstreuexperimente an großen Einkristallen der reinen Verbindungen durchgeführt. Die erzielten Ergebisse der Spin-Wellen-Anregung bzw. der Nachweis nicht-linearer Anregungen in den quasi eindimensionalen antiferromagnetischen Ketten von Na_2MnF_5 und $(ND_4)_2MnF_5$, die mittels eines thermischen bzw. eines kalten Dreiachsenspektrometers untersucht wurden, werden diskutiert. Außerdem werden Meßergebnisse der magnetischen Suszeptibilität und der elastischen Neutronenbeugung zur Beschreibung der magnetischen Struktur mitgeteilt. Aus der Breite des quasielastischen Signals wurde die Temperaturabhängigkeit der inversen Korrelationslänge ermittelt und hieraus die Solitonenaktivierungsenergien E_s/k = 65(3) K bzw. E_s/k = 81(3) K bestimmt, die in guter Übereinstimmung zu unseren Ergebnissen der hochauflösenden inelastischen Neutronenstreuexperimente stehen. Im Gegensatz hierzu ergiebt die Mössbauer-Spektroskopie den zweifachen Wert der Solitonenenergie, der durch Solitonen-Paaranregung oder Interbandanregung erklärt wird.

Introduction

One-dimensional (1-d) magnetic systems have attracted considerable interest in solid state physics. Based on topological reasons, short range order effects of interacting spins and non-linear excitations are essential in describing the spin dynamics of these compounds. One kind of non-linear excitations are the so-called solitons which are theoretically well examined [1]. The physical realization of a 1-d magnet are compounds in which the magnetic ions are arranged along chains. Consequently, the exchange interaction J along the chains is much stronger than the exchange constant J′ perpendicular to it. The ratio J′/J can be taken as a measure of the onedimensionality of a system. The existence of a nonvanishing interchain coupling J′ necessarily leads to a three-dimensional long range magnetically ordered state at sufficiently low temperatures. In any case, the typical features of 1-d magnetic behavior can be observed over a large temperature range above the ordering tempera-

* Prof. Dr. Jürgen Pebler
Fachbereich Chemie der Philipps-Universität
D-35032 Marburg
E-mail: pebler@chemie.uni-marburg.de

 DOI: 10.1002/zaac.200400009

ture. A recent review on the elementary excitations in prototypical examples of antiferromagnetic chain compounds can be found in *Mikeska* et al. [1] and references therein.

The fluoromanganates(III) are antiferromagnetic chain compounds which may serve as model systems for 1-d magnets as have been discussed by *Massa* et al. [2]. A common feature of all fluoromanganates(III) with the general formula $A^I_2/A^{II}MnF_5(H_2O)$ (with A=Li^+, Na^+, NH_4^+, ND_4^+, K^+, Rb^+, Cs^+, enH_2^{++}, Sr^{++} and Ba^{++}) is that they are built from infinite chains of trans corner-linked $[MnF_4F_{2/2}]^{2-}$ octahedra, with individual chains being seperated by alkaline (A^+) or earth alkaline (A^{2+}) ions. Due to the Jahn-Teller effect, the long axial Mn-F_{ax} bonds of the distorted $[MnF_4F_{2/2}]^{2-}$ octahedra all lie along the chain direction which yields a ferrodistortive arrangement. An increase in size of the counter-ion results in a widening of the (Mn-F_{ax}-Mn) bridging angle γ from 132.5 for Na_2MnF_5 to 180 for $Cs_2MnF_5(H_2O)$ respectively [3]. The coordination around Mn^{III} is very nearly axially symmetric (D_{4h}). The EPR-spectra for a single crystal of $(NH_4)_2MnF_5$ (space group Pnma, Z = 4) were found to be nearly isotropic with signals at g values of $g_\perp = 2.002$ and $g_\parallel = 1.997$ [4, 5].

A suitable Hamiltonian for the description of trans corner linked MnF_6 octaheder forming quasi one dimensional magnetic chains is given by

$$\hat{H} = \Sigma \{-2JS_iS_{i+1} + D\left(S_{i,z}^2 - \frac{1}{3}S_i(S_i+1)\right) + E\,(S_{i,x}^2 - S_{i,y}^2) - g\mu_B HS_i\} \quad (1)$$

The chain direction is along the z direction. The first term represents an isotropic Heisenberg exchange interaction between two neighboring spins with exchange constant -2J, D and E are the axial and rhombohedral anisotropy constants, respectively, and the last term is the Zeeman interaction in the presence of an external magnetic field. The single-ion-type anisotropy may arise from crystal potential. Since the equatorial Mn-F_{eq} distances in the plane perpendicular to the z axis differ only by less than 0.1 % we will neglect the orthorhombic anisotropy E (third term in eqn.(1)) in our discussion.

As has previously been shown for Mn^{III} chain compounds of the type $A^I_2/A^{II}MnF_5(H_2O)$ [6−7], it follows that $|D| \gg E$ and $|J| > |D|$. The model given in eqn. (1) is therefore a valid approximation to describe the properies of a 1-d Mn^{3+} magnetic system.

1 Mössbauer Spectroscopy

Previously, the spin dynamics of $A^I_2/A^{II}{}_1MnF_5(H_2O)$ (with A=Li^+, Na^+, NH_4^+, ND_4^+, K^+, Rb^+, enH_2^{++}, Sr^{++} and Ba^{++})has been studied on the 2 % ^{57}Fe doped compounds by means ofMössbauer spectroscopy [6−12]. In the following we focus our interest on the antiferromagnetic chain compounds of Na_2MnF_5 and $(ND_4)_2MnF_5$because we obtained for these compounds large single crystals enabling inelastic neutron scattering experiments.

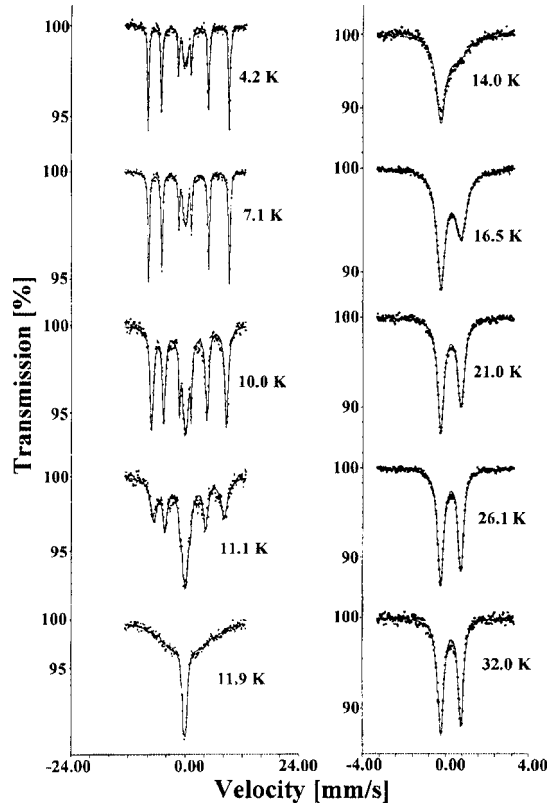

Fig. 1 Mößbauer spectra of $Na_2Mn_{0.98}Fe_{0.02}F_5$

In Fig.1 and Fig. 2 we present the temperature dependence of the Mössbauer relaxation spectra for the ^{57}Fe doped powder samples of Na_2MnF_5 and $(ND_4)_2MnF_5$, respectively. These relaxation spectra in a wide temperature range $T_N<T<3T_N$ were calculated and interpreted on the basis of the classical soliton theory [1, 13−15].

The detailed fitting procedure of the Mössbauer spectra is described in [8−12]. The characteristic Mössbauer parameter as quadrupole splitting and magnetic hyperfine field H are given in Table 1 for Na_2MnF_5 and $(ND_4)_2MnF_5$ in [7, 10]. The theoretical analysis of domain wall dynamics and solitons in magnetic chains with large local anisotropy D shows that, in a certain range below and above the critical temperature T_N, the density of π domain walls and their motion determines the spin autocorrelation function $\langle \mathbf{S}(0)\mathbf{S}(t)\rangle$, which is obtained by measurring the fluctuating hyperfine field $\mathbf{H}(t) \propto \mathbf{S}(t)$.

We want to emphasize, that a feature of our experimental results is the observation of two subspectra, each of which shows a separate relaxation mechanism. Approaching the magnetically split phase from above one observes the apparent coexistence of contributions from the paramagnetic and magnetically ordered phase. This transition is accompanied by slow and fast relaxation phenomena, which may be attributed to non-linear excitations of domain walls. This unsusual behaviour is observed e.g. in $(ND_4)Mn_{0.98}Fe_{0.02}F_5$ between 9 K and 13 K (Fig. 2). There appears a central asymmetric doublet due to faster relax-

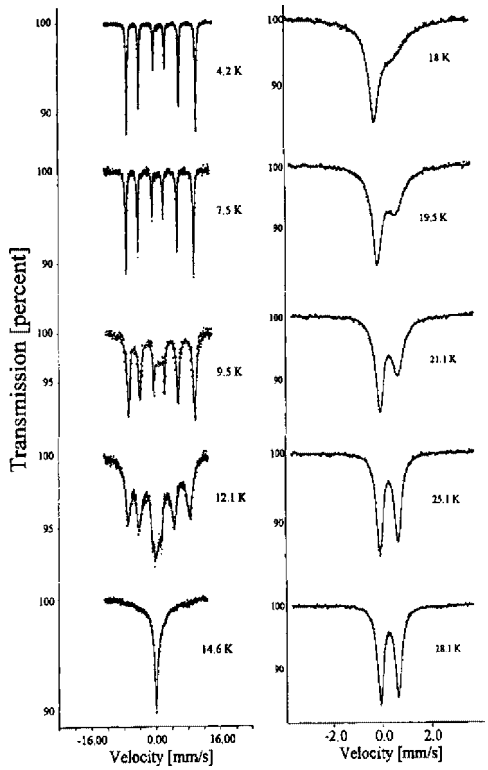

Fig. 2 Mössbauer spectra of $(ND_4)_2Mn_{0.98}Fe_{0.02}F_5$

Table 1 Experimentally determined parameters in the following order: Mössbauer parameters of the magnetic hyperfine field H_{hf}, the quadrupole splitting ΔE^Q at 4.2 K and the thermal activation energy E_A/k [7].

	H_{hf} kOe	ΔE^Q mm/s	E_A/k K
Na_2MnF_5	543(3)	1.118(7)	132(5)
$(ND_4)_2MnF_5$	525(3)	0.720(5)	162(5)

ation. Above 13 K, the intensity of the fast relaxing subspectrum becomes negligible, such that only a single spectrum (slow relaxing subspectrum) was sufficient to fit the experiment. The Mössbauer spectra were found to consist of two subspectra with equal static parameters, but different relaxation rates. These features are in common in all our samples studied by Mössbauer spectroscopy and were also observed for Fe^{II} compounds with strong anisotropy constants D by *de Jongh* and his group [13–15]. *Elmassalami* [15] identified the superposition of a slowly and a fast relaxing subspectrum with only one crystallographic metal site with the creation / annihilation of soliton pairs and intra-band solitons, respectively.

Finally, the Mössbauer spectra of $Na_2Mn_{0.98}Fe_{0.02}F_5$ and of $(ND_4)_2Mn_{0.98}Fe_{0.02}F_5$ could successfully be fitted by adopting the Blume Tjon relaxation model [16, 17], in which it is assumed that the hyperfine field jumps stochastically with a flipping rate Γ between the two possible values $+H_{hf}$ and $-H_{hf}$. This takes into account a time-dependent Hamiltonian. Thus, the hf interaction is replaced by a fluctuating effective field, and the increase in the fluctuating rate causes line broadening, asymmetric spectra, and related phenomena [14].

The spin fluctuation rate Γ is defined as

$$\Gamma = 2n_s v_s = v_s \xi^{-1} \tag{2}$$

where n_s is the soliton density

$$n_s = \sqrt{\frac{8}{\pi}} \cdot \frac{1}{d} \cdot \sqrt{\frac{E_s}{kT}} \exp\left(\frac{-E_s}{kT}\right) \tag{3}$$

v_s the soliton velocity

$$v_s = \frac{4\,|J|\,S}{\sqrt{\frac{E_s}{2kT}}} \tag{4}$$

d the width of a domain wall

$$d = \frac{4\,|J|S^2}{E_s} = \sqrt{\frac{|J|}{|D|}} \tag{5}$$

and E_s is the soliton energy

$$E_s = 4S^2 \sqrt{|D \cdot J|} \tag{6}$$

For the inverse correlation length ξ^{-1} (see eqn. (2)) it follows, that

$$\xi^{-1} = 2\,n_s = 2 \cdot \sqrt{\frac{8}{\pi}} \cdot \frac{1}{d} \cdot \sqrt{\frac{E_s}{kT}} \exp\left(\frac{-E_s}{kT}\right) \tag{7}$$

For higher temperatures a boundary condition is, that the inverse correlation $\xi^{-1}(T)$ for $T \rightarrow T(\chi_{max}) = |J|S(S+1)/k$ turns continuously to an istropic behoviour predicted by the Heisenberg model and given by

$$\xi_H^{-1} = -\ln\left[\coth\left\{\frac{2|J|S(S+1)}{kT} - \frac{kT}{J|S(S+1)}\right\}\right]. \tag{8}$$

The spin fluctuation rate Γ derived from the Mössbauer spectra can be expressed in the temperature range $T_N \leq T < |J|S(S+1)/k$ by

$$\Gamma = 2n_s v_s = \frac{2^5}{\sqrt{\pi}} J \cdot S \sqrt{\frac{D}{J}} \exp\left(\frac{-E_A}{kT}\right). \tag{9}$$

The activation energy $E_A \approx 2E_s$, as determined from the electronic flipping rate as a function of inverse temperature (see eq. (9)), was systematically found to be twice the energy E_s of a single soliton (see chapter 4), that is it corresponds instead to the energy of a soliton pair [15, 18]. The spin fluctuation rate changes from 10^6 to 10^{12} Hz in the temperature region $T_N \leq T \leq JS(S+1)/k$.

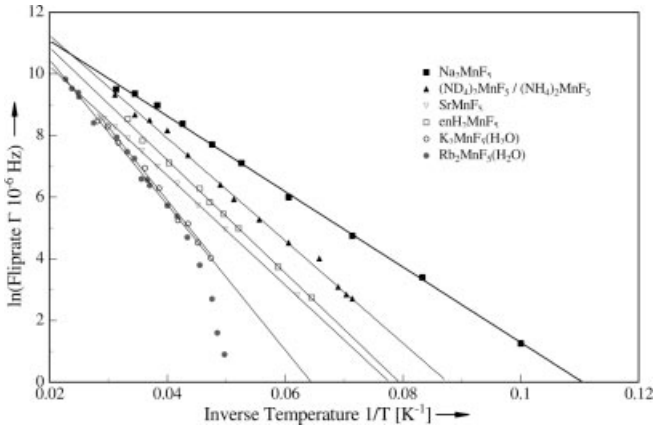

Fig. 3 Relaxation rate as a function of inverse Temperature for 2 % ^{57}Fe doped compounds of fluoromanganates (III).

For Na_2MnF_5 and $(ND_4)_2MnF_5$, the spin fluctuation rate ln(Γ(T)) versus the inverse temperature 1/T results in a thermal activation energy of $E_A/k = 132(5)$ K and $E_A/k = 162(5)$ K, respectively (see Table 1).

In Fig. 3 we present the relaxation rate versus inverse temperature for the ^{57}Fe doped compounds of the fluoromanganates(III) mentioned above. Additionally, we present measurements for $SrMnF_5(H_2O)$, enH_2MnF_5, $K_2MnF_5(H_2O)$, and $Rb_2MnF_5(H_2O)$ in Fig. 3 [7, 9−12].

2 Magnetic susceptibility

The magnetic studies on single crystals of Na_2MnF_5 (15 mg) and $(ND_4)_2MnF_5$ (20 mg), were performed with a SQUID magnetometer [19] in the temperature range 1.7-330 K and external fields in the range ±55 kG.

The experimental data $\chi_\parallel(T)$ for Na_2MnF_5 (χ_a) and $(ND_4)_2MnF_5$ (χ_b) represent the susceptibility values along the chain directions a and b and $\chi_\perp(T)$ are the perpendicular susceptibilities along the b and c or a and c axes respectively.

According to our discussions in [7] the magnetic susceptibility $\chi_\parallel$ of a 1-d antiferromagnetfollows to

$$\chi_\parallel(T) = \frac{Ng^2\mu_B^2 S(S+1)}{3kT} \cdot \frac{1-\exp\{-1/\xi\}}{1+\exp\{-1/\xi\}} . \qquad (10)$$

For $\xi \to 0$ and $T \to JS(S+1)/k \approx T(\chi_{max})$. $\chi_\parallel$ smoothly approaches the Curie law. The term $(S(S+1)/3)\cdot\exp(-1/\xi)$ represents the correlation function $\langle S_o^z S_r^z\rangle$. For Na_2MnF_5 the simulation of the magnetic susceptibility $\chi_\parallel$ by eqn. (10) is excellent. For $(ND_4)_2MnF_5$ the theoretical values according to eqn. (10) come close to the maximum of the magnetic susceptibiliy at $T = T(\chi_{max}) \cong S(S+1)|J|/k \cong 63$ K.

From our single crystal measurements we find that the spins are nearly antiparallel to the z axis (chain direction), but they have small canted components along the x or y axes (perpendicular to the chain direction) in the ordered state which produce a weak ferromagnetism. Previously, magnetic measurements on a single crystal of $(ND_4)_2MnF_5$ with the transverse detection unit of our SQUID system [19] showed that the ferromagnetic moment lies along the a axis for $T < T_N$. The canting angle φ (see Table 2) is caused by the local anisotropy producing a different preferential direction for the moments which are on different sublattices. This mechanism occurs when the local arrangement of the atoms around the sites of the magnetic ions are tilted with respect to each other.

The direction of local anisotropy for each sublattices is assumed to make an angle $\delta = (180 - \gamma)/2$ with the positive or negative z axis, where γ represents the bridging angles which amount to 132.5 and 139.5 for $Na_2MnF_5$and $(ND_4)_2MnF_5$, respectively [3]. If the preferred direction due to the anisotropy is the same for both sublattices ($\delta = 0$), the canting angle φ is evidently equal to zero. An increase of δ also increases the canting angle. If, on the other hand, the exchange interaction J is zero it is easily seen that $\delta = \varphi$.

To describe the spin behaviour one has, as mentioned above to solve the Hamiltonian of a magnetic chain for orthorhombic symmetry (see eqn. (1)). Due to the isotropy within the plane perpendicular to the chain axis ($E \cong 0$) we can construct the following expression for the susceptibility perpendicular to the chain axis. According to *Moriya* [20] the magnetic susceptibility of a canted system may be described by the sum of two contributions, namely an antiferromagnetic and a ferromagnetic part. Each of the contributions must be multiplied with an appropriate factor to take the value of the susceptibility component along the particular axis into account. For our description of the experimental susceptibility data on the weak ferromagnetic chain compounds, we used the correct theoretical expression for the 1-d Heisenberg model, multiplied with the factor $1\text{-}\sin^2\varphi$ [20]. Following [20], the ferromagnetic component can be described by a term $C/(T\text{-}T_N)$ multiplied with the factor $\sin^2\varphi$ where C is the Curie constant. In our case, for $\chi_\perp$ it follows that

$$\chi_\perp = \frac{Ng^2\mu_B^2 S(S+1)(1-\sin^2\varphi)}{3kT} \frac{1-\exp\{\xi^{-1}{}_H\}}{1+\exp\{\xi^{-1}{}_H\}} + \frac{Ng^2\mu_B^2 S(S+1)}{3k(T-T_N)} \sin^2\varphi \qquad (11)$$

where $\xi_H{}^{-1}$ represents the inverse correlation length (see eqn. (8)) in the Heisenberg model. The Figures 4 and 5 show the results for best fits of eqn. (11) to the experimental data for the perpendicular component of the magnetic susceptibility $\chi_\perp$. For Na_2MnF_5 and $(ND_4)_2MnF_5$ values of $T_N = 10.9$ K or 8.7 K and $\varphi = 5.1$ or 4.6 have been taken into account [21, 22]. Fixing as starting parameters the Néel temperature T_N and the exchange constant J the adjustable parameters are the anisotropy constant D, the soliton energy $E_s = 4S^2(|D||J|)^{1/2}$, and the spin canting angle φ. Finally we found from the best fit of eqn. (10) and eqn.(11) to the data of Na_2MnF_5: $D/k = -2.85(5)$ K, $J/k = -10.4(2)$ K, $E_s/k = 75(5)$ K, $\varphi = 5.0(5)$, $T_N = 10.9(3)$ K (see Fig. 8) and of $(ND_4)_2MnF_5$: $D/k = -2.85(5)$ K, $J/k = -10.4(2)$ K,

Table 2 Fit parameters for Na_2MnF_5 and $(ND_4)_2MnF_5$ in the following order: bridge angle γ by x-ray and neutron diffraction, the Nèel temperature T_N, the maximum of magnetic susceptibility $T(\chi_{max})$, the anisotropy constant D, the intrachain exchange constant J, the interchain exchange constant J′, and the canting angle φ derived from eqn. (11) [7].

	γ /	T_N /K	$T(\chi_{max})$ /K	D/k /K	J/k /K	J′/k /K	φ /
Na_2MnF_5	132.5	10.9(3)	53(2)	−2.75(4)	−8.8(2)	1.3 10^{-3}	5.0(5)
$(ND_4)_2MnF_5$	139.5	8.5(2)	63(2)	−2.74(5)	−10.3(1)	3.010^{-4}	4.6(3)

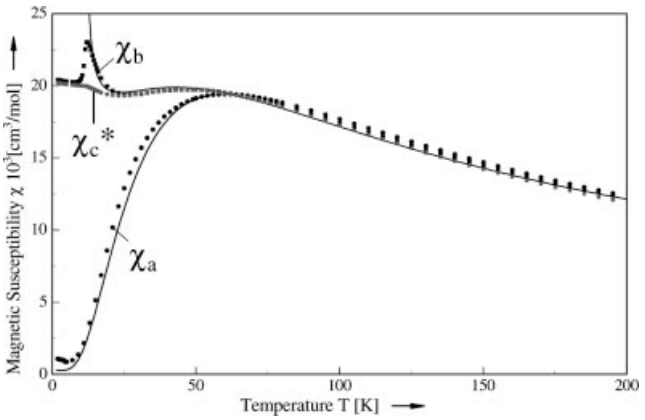

Fig. 4 Magnetic susceptibilities for the three crystallographic axes a, b and c* of a single crystal of Na_2MnF_5 are shown versus temperature. The solid lines are calculated from our model (see eqn. (10) and (11)).

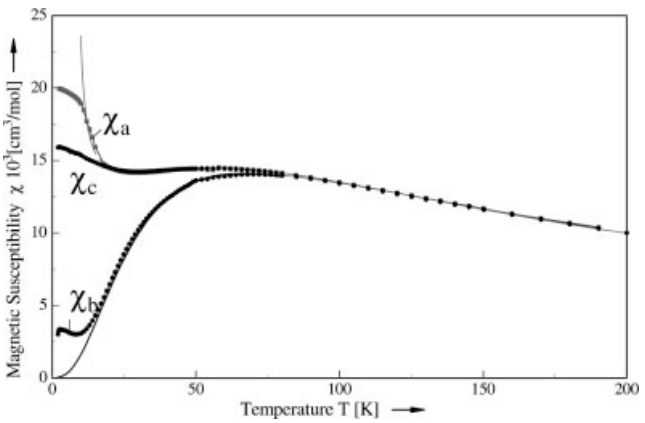

Fig. 5 Magnetic susceptibilities for the three axes a, b and c of a single crystal of $(ND_4)_2MnF_5$ are shown versus temperature. The solid lines are calculated from our model (see eqn. (10) and (11)).

$E_s/k = 85(3)$ K, $\varphi = 4.5^0$, $T_N = 8.5(2)$ K (see Figures 4 and 5).

Finally, we have recalculated the correlation lengths from eqn. (10) using the relation

$$\xi^{-1} = \ln\left\{\frac{1-A}{1+A}\right\} \quad \text{with} \quad A = \frac{3\chi_{\|}kT}{Ng^2\mu_B^2 S(S+1)} \tag{12}$$

Inserting in eqn. (12) the measued values $\chi_{\|}$, we obtain the temperature dependence of ξ^{-1} (T) derived from the magnetic susceptibility. These calculated values were inserted as points in Figure 14 for $(ND_4)_2MnF_5$.

3 Neutron experiments

In order to confirm this concept of non-linear excitations, we have independently performed neutron scattering experiments on the examples of $Na_2MnF_5$and $(ND_4)_2MnF_5$. The study of the non-linear spin dynamics requires first a precise knowledge of the exchange and anisotropy parameters of the Hamiltonian. Therefore we have determined the spin wave dispersion and the temperature dependence of the magnetic correlation length of Na_2MnF_5 and $(ND_4)_2MnF_5$. In a second step, we measured directly the non-linear spin excitations (solitons) by means of high resolution neutron spectroscopy.

3.1 Sample preparation and characterization of large single crystals

Large single crystals of Na_2MnF_5 (1.3 g) and $(ND_4)_2MnF_5$ (1.4 g) were synthesized by the evaporation method of a saturated solution of Na_2MnF_5 and $(ND_4)_2MnF_5$ in hydroflouric acid. Single crystal X-ray measurements at room temperature revealed for Na_2MnF_5 monoclinic structure characterized by space group $P2_1/c$ [23] (see Fig. 6) and for $(ND_4)_2MnF_5$ orthorhombic structure with space group Pnma [24, 25] (see Fig. 7). Neutron diffraction experiments confirmed the monoclinic structure of Na_2MnF_5 [21, 28] and the orthorhombic structure of $(ND_4)_2MnF_5$, and revealed the perfect homogeneity and excellent quality of the samples. The crystallographic parameters of Na_2MnF_5 are space group $P2_1/c$, lattice constants a = 7.719(1) Å, b = 5.236(1) Å, c = 10.862(2) Å, and monoclinic angle β = 109.0(1) . The brige angle (∠Mn-F-Mn) amounts to 132.5(2) . The crystallographic parameters of$(ND_4)_2MnF_5$ are space group Pnma, lattice constants a = 6.227(1) Å, b = 7.948(1) Å, c = 10.720(1) Å and a bridge angle (∠Mn-F-Mn) along the chain direction of 139.5(2) . On the same single crystal of $(ND_4)_2MnF_5$, *Massa* and *Paulus* [26] revealed by elastic neutron diffraction a structural phase transition into a monoclinic phase $P2_1/n$ at 239 K. In this phase the site symmetry at the Mn center is $\bar{1}$. The chains above and below the phase transition are very much the same [26].

3.2 Spin wave excitations

In a three-dimensional magnetically ordered compound, the spin dynamics is classically described by spin wave the-

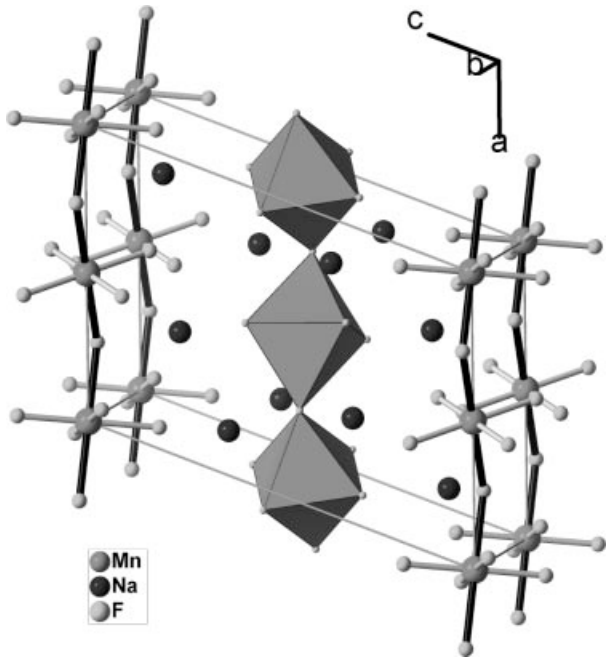

Fig. 6 Crystal structure at room temperature for Na_2MnF_5, studied by x-ray and neutron diffraction.

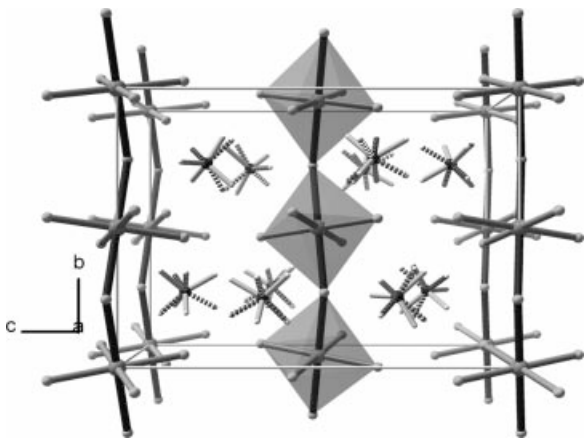

Fig. 7 Crytal structure at room temperature for $(NH_4)_2MnF_5$ and $(ND_4)_2MnF_5$, studied by X-ray and neutron diffraction

ory. In the present case of Na_2MnF_5 and $(ND_4)_2MnF_5$ one has again to solve the Hamiltonian of a magnetic chain in orthorhombic symmetry (see eqn. (1)).

The chain direction is along the z direction. In the present cases as already mentioned above we consider onlythe first two terms in eqn.(1), since for Mn^{III} chain compounds, it has been shown above that $J|>|D|$ and D>>E, and no field has been applied. In order to confirm the results of our model calculation of the magnetic susceptibility experiments, the first task is therefore to determine the exchange constant J and the axial anisotropy constant D of the Hamiltonian. This can be done by measuring the spin wave dispersion by means of neutron diffraction. The experiments

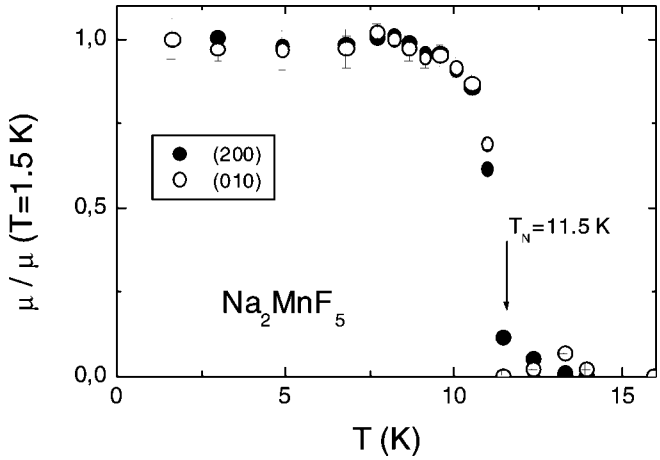

Fig. 8 Temperature dependence of the ordered magnetic moments of Na_2MnF_5, normalized to the saturation value at T=1.7 K.

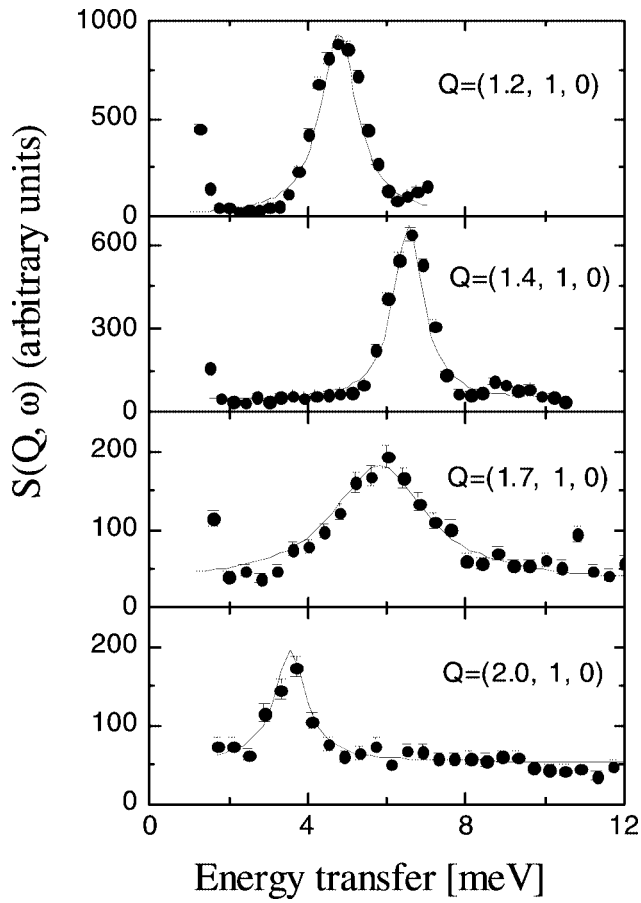

Fig. 9 Spin wave excitations of Na_2MnF_5 along the magnetic chain direction at T = 1.7 K. The varying excitation energies (peak positions) for different Q values nicely illustrate the spin wave dispersion [29].

have been performed on the thermal triple-axis spectrometer E7 at the Hahn-Meitner-Institute, Berlin and the spectrometer IN22 at the Institute Laue Langevin, Greno-

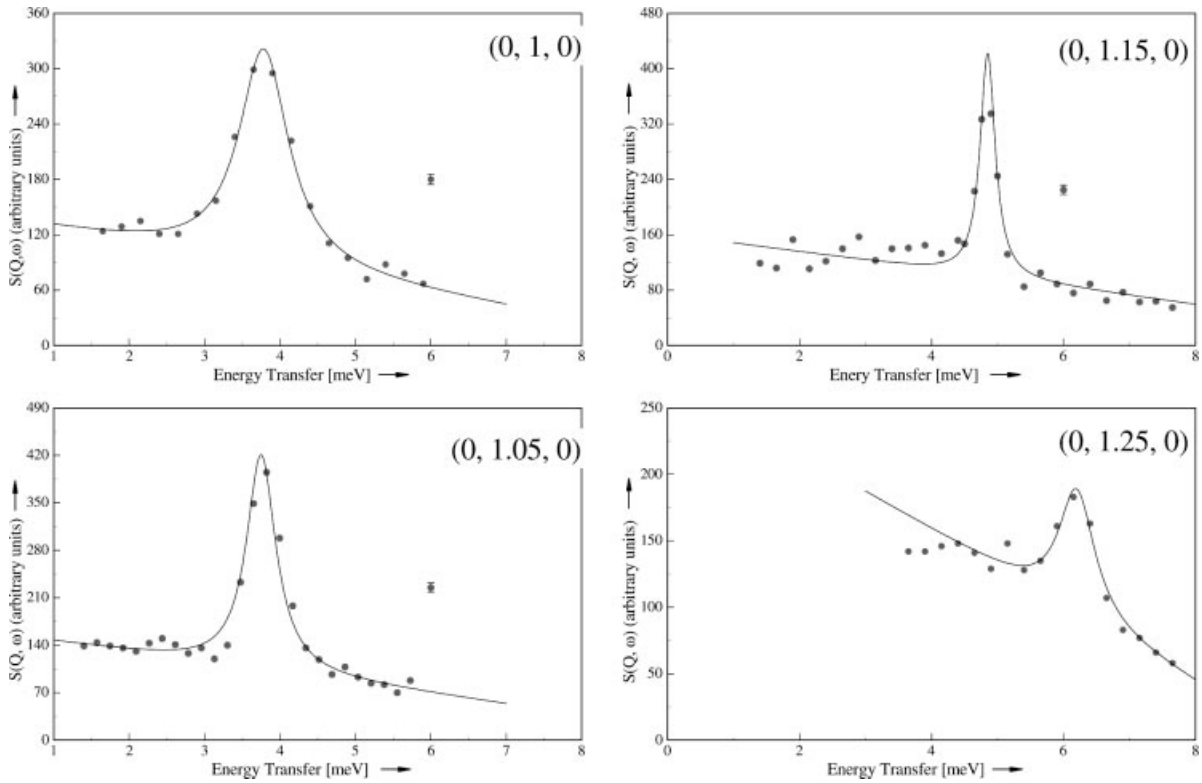

Fig. 10 Spin-wave excitations in $(ND_4)_2MnF_5$ at 1.7 K for different Q values at (0,1 +q, 0) along the chain direction.

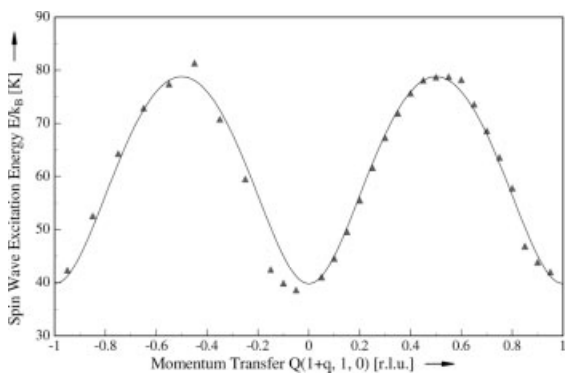

Fig. 11 Spin-wave dispersion of Na_2MnF_5 at T = 1.7 K. The solid line is a fit to the data according to eqn. (13) describing an antiferromagnetic chain. From the fit an energy gap of Δ_{magnon}/k = 39.8(2) K, exchange constant J/k = −8.5(1) K, and anisotropy constant D/k = −2.70(2) K were obtained.

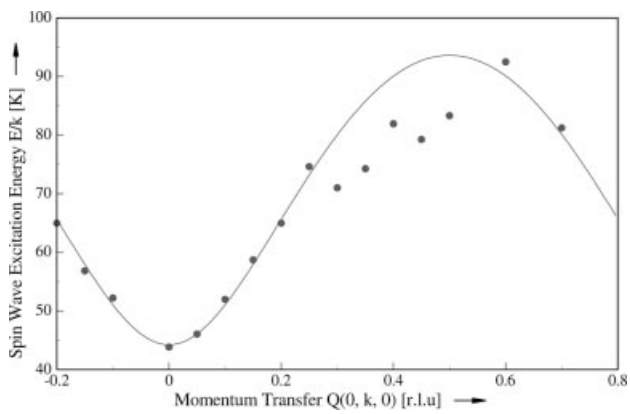

Fig. 12 Spin-wave dispersion of $(ND_4)_2MnF_5$ at T = 1.7 K. The solid line is a fit to the data according to eqn. (13) describing an antiferromagnetic chain. From the fit an energy gap of Δ_{magnon}/k = 44.3(6) K, exchange constant J/k = −10.3(1) K, and anisotropy constant Δ/k = −2.78(2) K were obtained.

ble. A standard configuration has been chosen with pyrolythic graphite monochromator and analyzer in constant final wave vector mode with k_f = 2.64 Å. The sample was mounted with the reciprocal lattice vectors a* and b* in the horizontal scattering plane. First we followed the temperature dependence of the magnetic Bragg intensities resulting in the Néel temperatures of T_N = 11.5(3) K for Na_2MnF_5 (e.g. see Fig. 8) and T_N = 8.5(4) K for $(ND_4)_2MnF_5$ in good agreement with our magnetic measurements.

The magnon dispersion relation along the chainshas been established by measuring the spin wave excitations throughout the Brillouin zone at T = 1.7 K well within the magnetically ordered state. Typical examples of the observed spin wave signals are shown in Figures 9 and10 for Na_2MnF_5 and $(ND_4)_2MnF_5$, respectively. The different width of the excitations are, at least to a major part caused by resolution effects. The data have been fitted by a single Lorentzian

Table 3 Magnetic properties of Na_2MnF_5 and $(ND_4)_2MnF_5$ as determined by measuring the spin wave dispersion relation at 1.7 K. Listed are the anisotropy constant D, the magnetic intra-chain constant J, the magnetic interchain constant J′ and the magnon energy gap Δ_{magnon} [21, 29].

	D/k	J/k	J′/k	Δ_{magnon}/k
Na_2MnF_5	−2.70(2)	−8.5(1)	$<2\ 10^{-2}$	39.8(2)
$(ND_4)_2MnF_5$	−2.78(2)	−10.3(1)	$< 10^{-3}$	44.3(6)

Table 4 Magnetic properties of Na_2MnF_5 and $(ND_4)_2MnF_5$, as determined by fitting the inverse correlation length (see eqn. (7)).

	D/k /K	J/k /K	E_s/k /K
Na_2MnF_5	−2.70(2)	−8.5(1)	65(5)
$(ND_4)_2MnF_5$	−2.85(5)	−10.7(2)	81(3)

line, convoluted with the instrumental resolution. The resulting dispersion curves show energy gaps of Δ_{magnon}/k = 39.8(2) K and Δ_{magnon}/k = 44.3(6) K and are displayed in Figures 11 and 12. The parameters J and D have been obtained by fits according to 1-d antiferromagnetic chains:

$$\eta\omega = [4S^2D^2 + 16S^2\,|J\|D| + 16(SJ)^2 \sin^2(\pi\cdot q_b)]^{1/2} \qquad (13)$$

The corresponding values J/k and D/k (see Table 3) are in very good agreement with the results of magnetic measurements. For the spin wave measurements perpendicular to the chain direction, no significant dispersion could be observed. This yields to an upper limit of the inter-chain exchange constants $|J'|/k < 2\ 10^{-2}$ and $|J'|/k < 10^{-3}$ K, respectively, thereby confirming the good one-dimensionality of the compounds. In order to check the possible influence of the inter-chain coupling onto the 1-d order, additional spin wave measurements along the chains have been performed at T = 20 K well above T_N. However, within the experimental accuracy no significant deviations could be observed as compared to the spin wave measurements at T = 1.7 K.

3.3 Magnetic correlation lengths

By removing the analyzer crystal from the triple-axis spectrometer, one can measure in an energy integrative mode, i.e. all neutrons are detected for a given scattering angle irrespective of their energy. A scattering geometry with k_f parallel to the chain direction has been chosen. From the width of the quasielastic scattering signal we have determined the temperature dependence of the magnetic correlation length of Na_2MnF_5 and $(ND_4)_2MnF_5$, as shown in Figures 13 and 14, respectively. For low temperatures, the inverse correlation length exhibits strong deviations from the Heisenberg / Fischer behavior shown as a dotted line in Figures 13 and Fig. 14. The exponential increase upon temperature is a typical feature for strongly anisotropic (Ising-like) systems. The temperature dependence of the inverse correlation length can be well described by classical soliton theory (solid line in Fig. 13 and Fig. 14), in which the inverse correlation length ξ^{-1} and the thermal soliton activation energy E_s are related by eqn. (7).

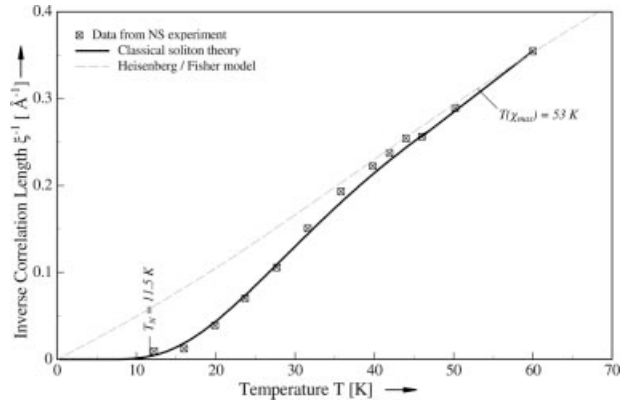

Fig. 13 Temperature dependence of the inverse correlation length of Na_2MnF_5. The full line corresponds to a fit according to classical soliton theory, whereas the dashed line represents a classical Heisenberg / Fisher behaviour. The Néel temperature and the temperature of the susceptibility maximum are indicated as well to illustrate the temperature region of the 1-d magnetic behaviour of Na_2MnF_5.

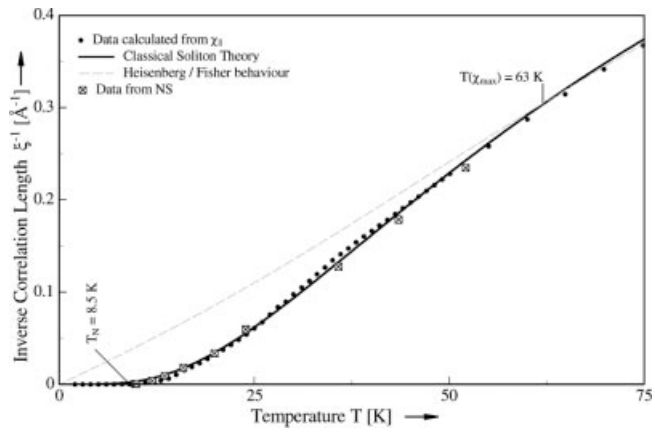

Fig. 14 Temperature dependence of the inverse correlation length of $(ND_4)_2MnF_5$. The experimental data from quasielastic neutron scattering (NS) could be satisfactorily fitted on the basis on the classical soliton theory (eqn. (7), solid line). The dash-dotted line represents (as in Fig. 13) the isotropic Heisenberg / Fisher model. Additionally, the ξ^{-1} values derived from magnetic susceptibility $\chi_\parallel$ (see eqn. (12)) were inserted.

To fit the experimental data with equation (7) we fixed as starting parameters the anisotropy constant D and the exchange constant J obtained by measuring the spin wave excitations or the magnetic susceptibility. Finally, the inverse correlation length ξ^{-1} was calculated for Na_2MnF_5 with parameters D/k = −2.70(2) K, J/k = −8.5(1) K, and the soliton energy E_s/k = 65(5) K [29]. For $(ND_4)_2MnF_5$ we find D/k = −2.85(5) K, J/k = −10.7(2) K, and E_s/k = 81(3) K [21, 27].

The temperature dependence of the inverse correlation lengths shown in Figures 13 and 14 are in very good agreement with the results of magnetic susceptibility measurements and Mössbauer spectroscopy on the iron-doped samples. This is a strong indication that the spin dynamics of Na_2MnF_5 and $(ND_4)_2MnF_5$ above the ordering temperatures is indeed dominated by the presence of soliton excitations.

3.4 Nonlinear excitations

High-resolution neutron diffractometry is the most direct experimental access to study non-linear magnetic excitations. Neutron scattering by solitons gives rise to a weak quasielastic intensity hidden by a large incoherent elastic background signal. Therefore, high neutron flux, high resolution, and large single crystalline samples of high quality are the prerequisites for a successful experimental determination of soliton excitations.

In order to study the soliton dynamics directly, we have performed high resolution inelastic neutron scattering experiments. The experimental difficulties of these measurements are twofold. First, any soliton signal is very weak in intensity. This requires high neutron flux and big single crystalline sample and high quality (see above). As mentioned above, the investigated samples of Na_2MnF_5 and $(ND_4)_2MnF_5$ were single crystals of 1.3 g and 1.4 g masses and of excellent quality. The second difficulty is that the scattering intensity due to solitons appears close to zero energy transfer. The desired signal is therefore hidden below a strong incoherent background and its detection needs high instrumental resolution contradicting the requirement of high flux.

The neutron scattering experiments have been performed on the cold triple-axis spectrometer V2, located at the Hahn-Meitner-Institut, Berlin and on the cold three-axis spectrometer IN12, located at the Institute Laue Langevin, Grenoble. In order to determine the incoherent background properly, additional measurements at $T = 1.7$ K deep within the magnetically ordered states of Na_2MnF_5 and $(ND_4)_2MnF_5$ and at $T=70$ K (within the purely paramagnetic phase) have been performed. After the background corrections, residual weak quasielastic signals could be observed. The decreasing intensity upon increasing momentum transfer confirms its magnetic origin. The data could be fitted with a single Lorentzian line or a pseudo-Voigt profile, convoluted with the instrumental resolution, as shown for Na_2MnF_5 in Figure 15. The width of the signal strongly increases with increasing temperature. The classical soliton model describing a non-interacting soliton gas predicts an exponential temperature dependence of the line width upon temperature. From the knowledge of the anisotropy and exchange constants J and D, as derived by the measurements of the spin wave dispersion and single crystal susceptibility, the only adjustable parameter is the soliton activation energy E_s. Therefore, attributing our measured quasielastic scattering signals solely to soliton excitations, the observed temperature dependences of the linewidth determines the soliton activation energy, as displayed for Na_2MnF_5 in Figures 15 and 16.

The slopes of $\ln[\Gamma(T)]$ versus the inverse temperature 1/T correspond for Na_2MnF_5 and $(ND_4)_2MnF_5$ to soliton activation energies of $E_s/k = 65(5)$ K and $E_s/k = 81(5)$ when employing a single Lorentzian line and to $E_s/k = 60(5)$ K and $E_s/k = 76(5)$ K, respectively, when performing the fits by a pseudo-Voigt profile (as shown in Fig. 15).

From a physical point of view the essential information contained in $S(Q,\omega)$ – see Figure 15 – is that the antiferromagnetic Bragg peak, which is present at 1.7 K and $T < T_N$, is broadened owing to the presence of solitons for $T > T_N$. The broadening is described quantitatively by the inverse correlation length $\xi^{-1} = 2n_s$ (see eqn. (7)) where n_s represents the soliton density. It is thus the width of this peak, which is the signature of antiferromagnetic solitons.

4 Discussion and Conclusion

We have investigated the 1-d magnetic behavior of Na_2MnF_5 and $(ND_4)_2MnF_5$ by means of Mössbauer spectroscopy, magnetic susceptibility measurements and various neutron scattering techniques. The results are given in the Tables 1-5. The exchange constants J and anisotropy constants D, as determined by measuring the spin wave dispersion, as well as the temperature dependence of the magnetic correlation length are in very good agreement with the results of single crystal susceptibility measurements and Mössbauer spectroscopy on 2 % ^{57}Fe doped compounds. The temperature dependent magnetic correlation lengths for Na_2MnF_5 and $(ND_4)_2MnF_5$ are consistent with soliton activation energies of $E_s/k = 65(5)$ and $E_s/k = 81(5)$ K, respectively, which have been confirmed by direct measurements of the soliton excitations in high-resolution neutron scattering experiments (see Table 5).

The slightly smaller values of the magnetic ordering temperature T_N of $(ND_4)_2MnF_5$ as compared to Na_2MnF_5 are due to a larger interchain metal distances [3, 21]. The larger values of the intrachain exchange constant J and the soliton activation energy E_s of $(ND_4)_2MnF_5$ as compared to Na_2MnF_5 are due to the experimental results that the exchange interaction increases for 1-d fluoromanganates(III) with increasing bridge angle γ as $J/k = J_0/k \cos^2\gamma$ with $J_0/k \approx 18$ K [3, 30]. Fixing the anisotropy constants D for fluoromanganates(III) in eqn.(6) the activation (soliton) energy E_s would be proportional to $\cos\gamma \sqrt{J_o}$.

However, there is a remarkable difference of the resulting soliton activation energies on the basis of our neutron scatteringdata compared to the Mössbauer spectroscopy. The Mössbauer measurements gives within the range of statisical error twice the value of the soliton energy as determined by neutron diffraction, as evident from Tables 1 and 5 (see also Figure 17). In connection with nonlinear excitations, it is interesting to considerthe dispersion behaviour of an antiferromagnetic Ising-type chain. *Nagler* et al. [18] distinguish between different spin contributions to two dif-

Table 5 Comparison of the results of soliton activation energies for Na_2MnF_5 and $(ND_4)_2MnF_5$, as determined by high-resolution neutron spectroscopy with different fitting procedures and by Mössbauer spectroscopy

	soliton energy E_s/k (single Lorentzian line)	soliton energy E_s/k (pseudo-Voigt profile)	soliton energy $E_s/k = 1/2E_A/k$ Mössbauer effect (see Tab.1)
Na_2MnF_5	65(5)	60(5)	66(5)
$(ND_4)_2MnF_5$	81(5)	76(5)	81(5)

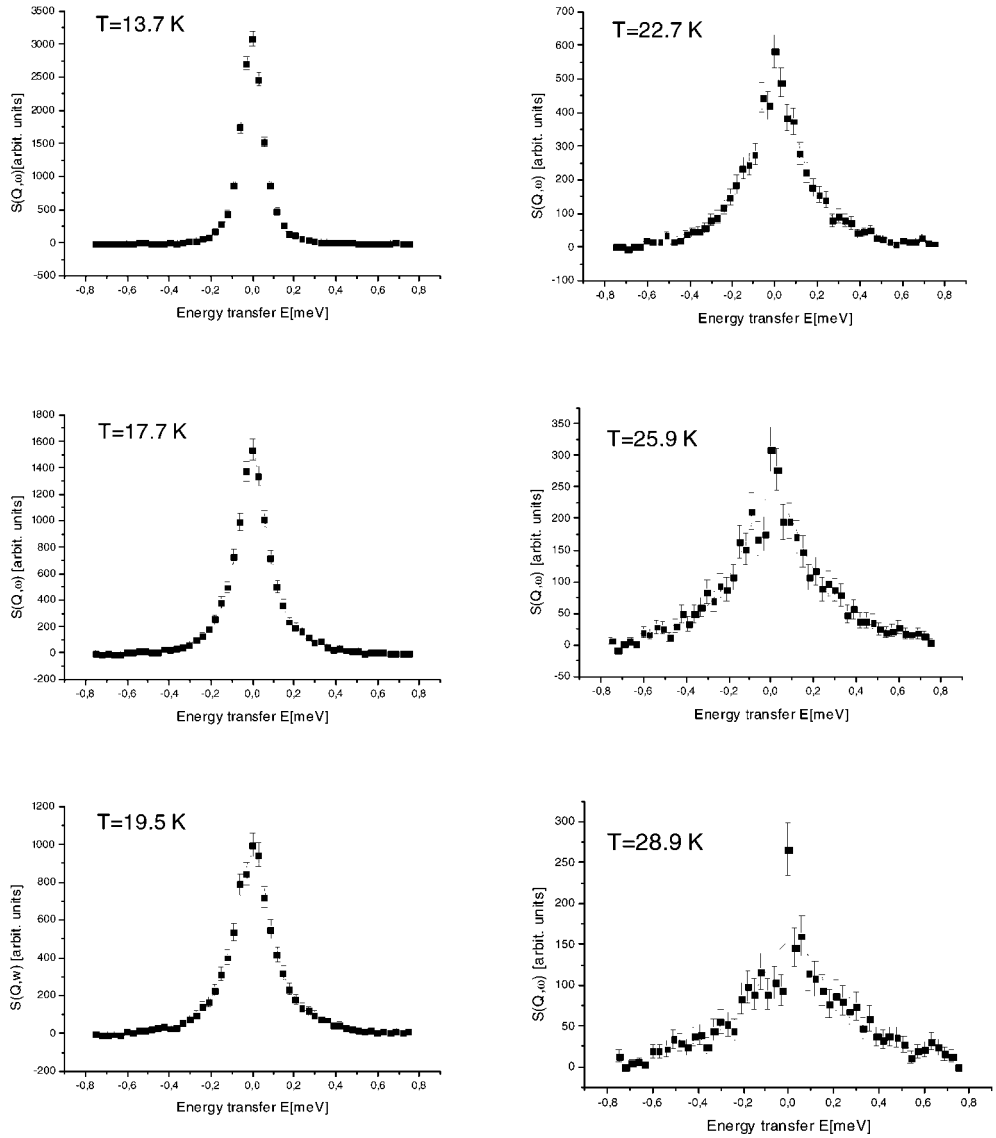

Fig. 15 Residual quasielastic scattering signal S(Q, ω) of Na_2MnF_5 for various temperatures, attributed to the presence of soliton excitations.

ferent modes: (i) the interband $\omega \approx \pm 2J$ excitations (spin wave-type excitations) and (ii) the soliton excitations or intraband ($\omega \approx 0$) excitations. The first kind excites the chain from the ground state with a soliton pair excitation energy $\propto 2E_s$ (E_s corresponds to the single soliton energy, see. eqn. (9)). Since the soliton pair excitations are thermally activated, a coupling between the spin system and the phonon bath is required which may be provided by spin-orbit coupling. In the Mössbauer experiments of Na_2MnF_5 and $(ND_4)_2MnF_5$, the dominating relaxation mechanism appears to be interband solitons. The second kind of excitations couples two states in the continuum band around an energy $2E_s$. In this case the dominating relaxation mechanism appears to be intraband solitons. Since solitons can not be excited by inelastic neutron scattering, only the spins of the thermally excited solitons will contribute to the

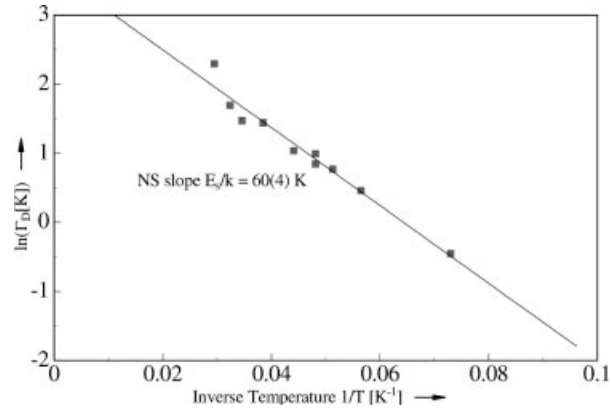

Fig. 16 Semilogarithmic plot of the linewidth of the quasielastic neutron scattering signal (NS) vs the inverse temperature of Na_2MnF_5. The slope determines the single soliton activation energy.

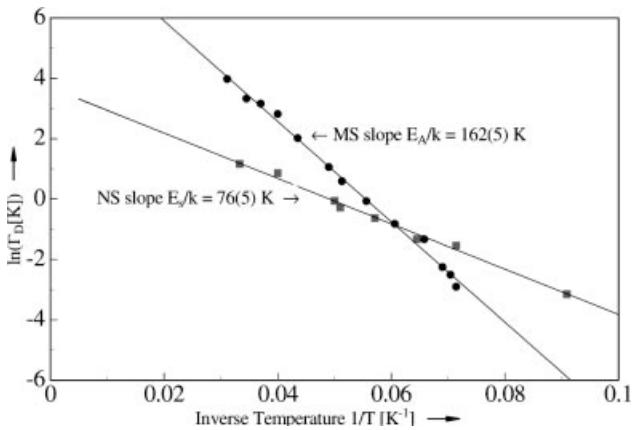

Fig. 17 Semilogarithmic plot of the linewidth of the quasielastic scattering neutron signal (NS) vs the inverse temperature of $(ND_4)_2MnF_5$. The slope determines the soliton activation energy. For comparison, the results of Mössbauer spectroscopy (MS) are also shown. As evident from the figure, the two different experimental techniques lead to remarkably different activation energies (see text).

central peak around $\omega \approx 0$. Therefore, with increasing temperature T the soliton density experimentally increases like $\propto \exp(-E_s/kT)$ (see eqn. (3)) as it is observed in our inelastic neutron scattering studies. Our results are in agreement with the interpretation of Mössbauer data on pure linear-chain Fe^{II} compounds by *de Jongh* and co-workers [13–15].

Most recently we have studied the double chain structure $(imidH)_2[Fe_2(ox)F_6]$ with weak Ising-type anisotropy by means of Mössbauer spectroscopy. In this Fe^{3+} chain-like compound with S=5/2 the local anisotropy is of dipolar origin (D/k = 0.15 K) and the anisotropy energy DS^2 is much smaller than the 3-d ordering energy kT_N. Consequently, an activated soliton excitation is not be observed above T_N = 14.5 K. Therefore, static domain walls must be already excited at lowest temperatures. Indeed, the striking result of our study [31] is the observation that the dominating ralaxation mechanism appears to be these intraband solitons which are proportional to $\exp(-E_s/kT)$ as it was supposed by *Elmassalami* [15] and found as the fast relaxing subspectrum (second subspectrum) in the fluoromanganates(III) studied above.

Acknowledgment. This work has been supported by the Bundesministerium für Bildung, Wissenschaft, Forschung und Technologie (BMBF Grant Nos. PE04.22k and FK:03-BA4MR-5), and the Fonds der Chemischen Industrie. Also, financial support under contract No. 03-LO5Akl-5 (BEO, Verbund IV) is gratefully acknowledged.

References

[1] For a review of experimental and theoretical work on 1-D magnetism, see for example: H. J. Mikeska and M. Steiner, *Adv. Phys.* **1991**, *40*, 161.
[2] W. Massa, M. Molinier, J. Pebler, *J. Fluorine Chem.* **1995,** *72*, 171.
[3] J. Pebler, W. Massa, H. Lass, B. Ziegler, *J. Solid State Chem.* **1987,** *71*, 87.
[4] J. M. Dance, private communication, **1987**.
[5] A. Krimmel, H.-A. Krug von Nidda, A. Loidl, M. Mangold, J. Pebler, *J. Phys. Condens. Matter***2002**, *14*, 4585.
[6] C. Frommen, Diplomarbeit, Univ. Marburg **1991**.
[7] J. Pebler, C. Frommen, M. Mangold, W. Treutmann, *Z. Naturforsch.* **1999**, *54a*, 317.
[8] J. Pebler, W. Massa, F. Hahn, D. Babel, "Organic and Inorganic Low-Dimensional Crystalline Materials", NATO ASI Series, Plenum Press, **1987**.
[9] J. Pebler, *Inorg. Chem.* **1989**, *28*, 1038.
[10] C. Frommen, J. Pebler, *Hyperf. Interact.* **1995**, *96*, 51.
[11] C. Frommen, L. Schröder, U. Bentrup, W. Massa, J. Pebler, *Z. Naturforsch.* **1995**, *50b*, 1227.
[12] C. Frommen, M. Mangold, J. Pebler, *Z. Naturforsch.* **1996**, *51a*, 939.
[13] L. J. de Jongh, *J. Appl. Phys.* **1982**, *53*, 8018.
[14] H. J. M. de Groot, PhD Thesis, Kammerling Onnes Laboratory, Univ. Leiden, The Netherlands **1987**.
[15] M. Elmassalami, Thesis, Univ. Leiden, The Netherlands **1989**; M. Elmassalami, H. H. A. Smit, H. J. M. de Groot, R. C. Thiel, L. J. de Jongh, in *Prog. in Phys.* 23, "Magnetic Excitations and Fluctuations II, eds. U. Balucani, S. W. Lovesey, M. G. Rasetti, V. Tognetti, p. 178, Springer Verlag, Berlin, 1987.
[16] M. Blume, J. A. Tjon, *Phys. Rev.* **1968**, *B165*, 446.
[17] M. Blume, J. A. Tjon, *Phys. Rev.* **1968**, *B174*, 351.
[18] S. E. Nagler, W. J. L. Buyers, R. L. Armstrong, B. Briat, *Phys. Rev.* **1983**, *B28*, 873.
[19] from QUANTUM DESIGN, San Diego, U.S.A. **1991**.
[20] T. Moriya, *Phys. Rev.* **1960**, *120*, 91.
[21] A. Krimmel, R. Stief, J. Pebler, R. Schneider, J.-U. Hoffmann, D. Hohlwein, D. Toebbens, to be published in *Phys. Rev. B* **2004**.
[22] R. van de Kamp, A. Krimmel, M. Mangold, J. Pebler, *Phys. Rev.* **2000**, *B61*, 15221.
[23] W. Massa, *Acta Crystallogr.* **1986**, *C42*, 644.
[24] R. Sears, J. L. Hoard, *J. Chem. Phys.* **1969**, *50*, 1066.
[25] F. Hahn, Thesis, Univ. Marburg, **1989**.

[26] W. Massa and W. Paulus, private communications. The characterization by neutron diffraction was performed at the ORPHEE reactor in Saclay
[27] M. Steiner, M. Winkelmann, M. Baehr, D. Hohlwein, A. Krimmel, Ch. Frommen, M. Mangold, J. Pebler, *Physica* **1998**, *B241-243*, 555.
[28] P. Nunez, J. Darriet, P. Bukovec, A. Tressaud, P. Hagenmuller, *Mat. Res. Bull*. **1987**, *22*, 661.
[29] A. Krimmel, R. Stief, J. Pebler, L.-P. Regnault, M. Ohl, *Phys. Rev.* **2003**, *B67*, 24405.
[30] A. Ahmadi, R. Stief, W. Massa, J. Pebler, *Z. Anorg. Allg. Chem*. **2001**, *627*, 869.
[31] Roland Leo, Werner Massa, Jürgen Pebler, to be published in *J. Fluorine Chem*. **2004**.

